Latest results from the EU project AVATAR: Aerodynamic modelling of 10 MW wind turbines

J.G. Schepers O. Ceyhan and K. Boorsma[1], A. Gonzalez, X Munduate, O Pires[2], N.. Sørensen[3], C. Ferreira[4], G Sieros[5], J. Madsen[6], S. Voutsinas[7], T. Lutz[8] G. Barakos and S. Colonia [9], H. Heißelmann[10], F. Meng[11], A. Croce[12]

[1]ECN, Westerduinweg 3, 1755 LE Petten, The Netherlands
[2]CENER, C/ Ciudad de la Innovación 7, 31621 Sarriguren, España
[3]DTU, Frederiksborgvej 399, 4000, Roskilde, Denmark
[4]TU Delft, Kluyerweg 1, 2629 HS Delft, The Netherlands
[5]CRES, 19th km Marathonos Ave., 19009 Pikermi Attiki, Greece
[6]LM Wind Power, AageSkouboesvej, 6640, Lunderskov, Denmark
[7]NTUA, P.O. Box 64070, 15710 Zografou, Athens, Greece
[8]University Stuttgart, Pfaffenwaldring 21, 70569 Stuttgart, Germany
[9]University of Glasgow, School of Engineering, Glasgow, Scotland, UK
[10] ForWind - Institute of Physics, University of Oldenburg,, 26129 Oldenburg, Germany
[11]Fraunhofer IWES, Am Seedeich 45, 27572, Bremerhaven, Germany
[12]Polimi, Via La Masa 34, 20156 Milano, Italy

schepers@ecn.nl

Abstract. This paper presents the most recent results from the EU project AVATAR in which aerodynamic models are improved and validated for wind turbines on a scale of 10 MW and more. Measurements on a DU 00-W-212 airfoil are presented which have been taken in the pressurized DNW-HDG wind tunnel up to a Reynolds number of 15 Million. These measurements are compared with measurements in the LM wind tunnel for Reynolds numbers of 3 and 6 Million and with calculational results. In the analysis of results special attention is paid to high Reynolds numbers effects. CFD calculations on airfoil performance showed an unexpected large scatter which eventually was reduced by paying even more attention to grid independency and domain size in relation to grid topology. Moreover calculations are presented on flow devices (leading and trailing edge flaps and vortex generators). Finally results are shown between results from 3D rotor models where a comparison is made between results from vortex wake methods and BEM methods at yawed conditions.

1. Introduction, objective and approach

This paper presents the most recent results from the EU FP7 project AVATAR (AdVanced Aerodynamic Tools of lArge Rotors). AVATAR was initiated by EERA (European Energy Research Alliance) and started in November 2013. The project will last 4 years and is carried out in a consortium with 11 research institutes and two industry partners.

- Energy Research Centre of the Netherlands, ECN (Netherlands, coordinator)
- Delft University of Technology, TU Delft (Netherlands)
- Technical University of Denmark, DTU (Denmark)
- Fraunhofer IWES (Germany)
- ForWind - Institute of Physics, University of Oldenburg (Germany)
- University of Stuttgart (Germany)
- National Renewable Energy Centre, CENER (Spain)
- University of Glasgow (UK)
- Centre for Renewable Energy Sources and Saving, CRES (Greece)
- National Technical University of Athens, NTUA (Greece)
- Politecnico di Milano, Polimi (Italy)
- General Electric, GE (Germany)
- LM Wind Power (Denmark)

The focus of the AVATAR project is the aerodynamic modelling of large wind turbines with a rated power of 10 MW or more (denoted as 10MW+ turbines). The deployment of such large scale turbines is mainly thought to be off-shore. This is due to the significant costs of the installation, support structure and grid connection for offshore wind energy, that make the share of the turbine hardware in the overall investment cost much less than for an on-shore turbine by which new blade technologies become more economically viable. Moreover, increasing the ratio between rotor diameter and installed generator power, i.e. a lower specific power, yields a higher capacity factor leading to more operating hours in full power and hence less variability in wind power and more effective use of the power transport cables, which is a major advantage for utilities. Other Cost of Energy (CoE) drivers that motivate a growing rotor area are the plain economies of scale with increasing energy capture per foundation.

The challenge though, is that rotor designs of such large scale largely fall outside the validated range of current state-of-the-art aerodynamic and aero-elastic tools in various aspects: Very large blades operate at high Reynolds numbers in view of the Reynolds number dependency on scale. The Reynolds number may even be enhanced by the higher tip speeds which could apply for off-shore applications in view of the fact that such turbines operate far from populated areas by which they do not suffer from noise requirements. This enables operation at high tip speed to take advantage of the associated reduced drive train loads. Generally, the effects of these high Reynolds numbers are uncertain and not enough validated, which is also true for the compressibility effects which may result from the higher tip speeds;
Other uncertainties result from the thick(er) airfoils which are applied on large rotors, the effects of which need to be assessed in terms of aerodynamic performance. Moreover the increased flexibility of large rotors leads to larger deflections and a more pronounced non-linear aeroelastic behaviour with unknown aerodynamic implications.
Further complications may result from possible implementation of active and/or passive flow devices which could be expected on large turbines to enhance power production and reduce load levels. Such devices are hard to model in 2D, and even harder in 3D rotating conditions.

The aim of AVATAR is to improve and validate aerodynamic models, and to ensure their applicability for 10MW+ turbines with and without flow devices, and with and without aero-elastic implications. Thereto, a wide variety of aerodynamic models is considered, ranging from low complexity/computational efficient models (i.e. Blade Element Momentum - BEM) to high fidelity computationally demanding models (e.g. Computational Fluid Dynamics - CFD), with intermediate

models (e.g. free vortex wake models) also included. This enables an improvement of the low complexity, fast tools via calibration of their results using high fidelity models. Furthermore, the improvement and validation of models is based on suitable experimental data. Amongst others, measurements on a DU 00-W-212 airfoil at Reynolds numbers between 3 and 15 Million were taken in the pressurized DNW HDG wind tunnel in Göttingen. In addition, the project partner LM provided measurements on the same airfoil taken in their tunnel and another project partner ForWind provided data under controlled turbulent conditions from their tunnel. Moreover, several other wind tunnel data sets for flow devices (vortex generators, dynamic/static flaps and root spoilers) are available.
The model assessment is carried out on two 10 MW reference wind turbines (RWT's), one originating from the INNWIND.EU project, and another one designed in AVATAR.
The latter is based on the INNWIND.EU reference turbine [1] but is more challenging in terms of aerodynamic modelling. Aspects like airfoil thicknesses, Reynolds and Mach numbers etc. are pushed towards the limits, i.e.towards more extreme values though still realistic to expect for future commercial applications.

2. AVATAR RWT

In this section the design of the AVATAR 10 MW reference wind turbine (RWT) is described.
This wind turbine took the characteristics of the INNWIND.EU reference design as a basis, the main characteristics of which are presented in the second column of table 1.
The resulting characteristics of the AVATAR reference turbine are then presented in the third column.

Table 1. Basic reference turbine characteristics: AVATAR RWT versus INNWIND.EU RWT.

	INNWIND.EU	AVATAR
Rated power	10 MW	10 MW
Rotor diameter	178.3 m	205.8 m
WTPD	400 W/m^2	300 W/m^2
Axial induction	~0.3	~0.24
Rotor speed	9.8 rpm	9.8 rpm
Tip speed	90 m/s	103.4 m/s
Hub heigt	119 m	132.7 m

It can be noted that the rated power of both the INNWIND.EU RWT and the AVATAR RWT is 10 MW but the diameter of the AVATAR turbine was increased from 178.4 to 205.76 meters reducing the Wind Turbine Power Density (WTPD) from 400 to 300 W/m^2. Table 1 shows another important difference between the INNWIND.EU RWT and AVATAR RWT , i.e. the axial induction factor that is approximately 0.3 for the INNWIND.EU RWT and 0.24 for the AVATAR RWT. The motivation for a low induction rotor is explained in figure 1 (See also [2]) which shows the power coefficient C_P and the axial force coefficient C_{Dax} (i.e. a measure for the aerodynamic load level) as function of axial induction factor according to the relations from the momentum theory:

$C_P = 4a(1-a)^2$ (1)
$C_{Dax} = 4a(1-a)$ (2)

Expression [1] leads to the well known maximum power coefficient of 16/27 from Betz at an axial induction factor of 1/3. Still it could be beneficial to design for a lower induction factor i.e to reduce the power coefficient slightly, since figure 1 shows a relatively flat behavior of C_P around a = 1/3 going together with a relatively strong dependency of C_{Dax}. The resulting strong reduction in axial

force coefficients then enables a larger rotor diameter at the same rotor forces since F_{ax} scales with C_{DAx} R^2 . On the other hand, the increase in rotor diameter overcompensates the small reduction in C_P leading to a higher power level due to the fact that P scales with C_P R^2.

Studies performed in AVATAR [3] show that the larger diameter could potentially lead to a higher energy production in the order of 5% for a representative wind climate where key aerodynamic load levels are maintained. It is noted that the initial power curve calculations with blade flexibility showed a lower power curve for the AVATAR blade due to strong torsional deformation. After increasing the torsional stiffness the power curve of the AVATAR turbine became higher again.

In Figure 2 the conditions along the blade are presented which shows Reynolds number up to 20 M far beyond the value of 6M for which most of the current models are validated for. Moreover, the tip Mach number, of the order of 0.3, enters the regime of slight compressibility while current models, generally, assume incompressible conditions.

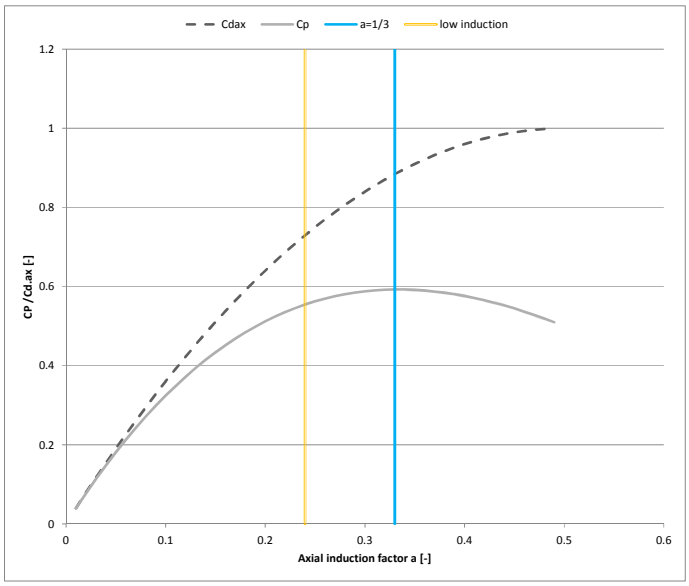

Figure 1. Power and axial force coefficient as function of axial induction factor. Lines for maximum power coefficient (a=1/3) and low induction are indicated

Although static rotor loads were maintained on the AVATAR RWT, the larger rotor diameters obviously yields higher mass loads. These higher mass loads were reduced by using (more expensive) carbon instead of glass for several components. Indicative results from [4] (assuming carbon three times more expensive than glass) yields a 2 % reduction in LCOE if the 100 INNWIND.EU turbines in a 1 GW off-shore wind farm are replaced by 100 AVATAR turbines. An additional advantage of the AVATAR turbine was found to be the reduced wake effects associated to the lower induction which yield an optimal Wind Farm Power Density of 3.4 MW/km^2 versus 3.1 MW/km^2 for the wind farm with INNWIND.EU turbines.

It is emphasized that even though the above mentioned (indicative) results show potential for a low induction rotor, it is not the aim of AVATAR to promote any concept: AVATAR's main aim is to prepare the aerodynamic modelling in wind turbine design codes for all possible future concepts with the low induction concept being one of the feasible options. In this context the importance of a low induction concept lies in the larger rotor diameter, the associated higher tip speed and the associated high Mach number and large Reynolds number which pushes the aerodynamic modelling towards the

limit. On the other hand, the lower induction values of the AVATAR turbine makes the concept less challenging in terms of induction modelling.

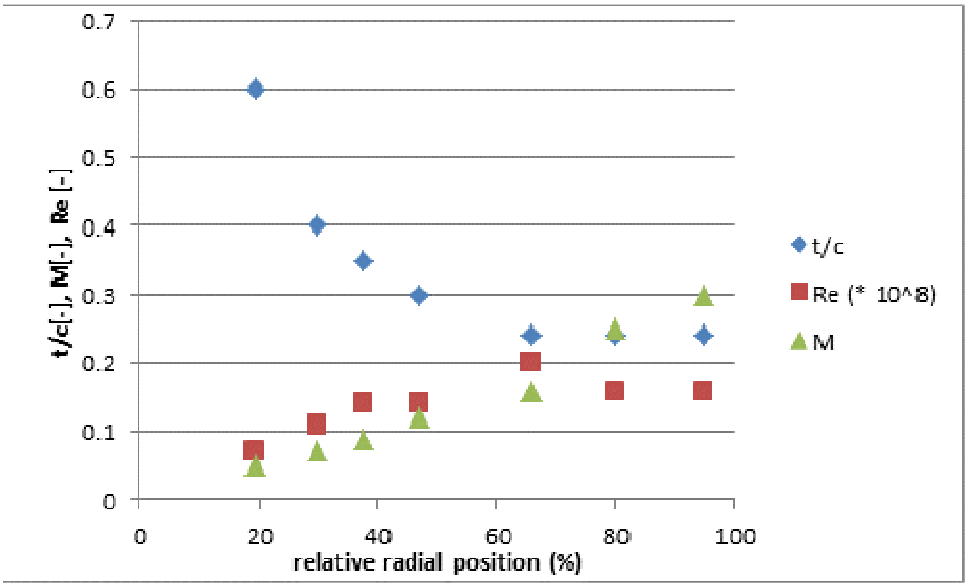

Figure 2. Operational conditions along the AVATAR blade.

3. Wind tunnel measurements

3.1. Wind tunnel measurements: Introduction

Within AVATAR several airfoil wind tunnel measurements are performed with and without flow devices. Unique measurements were carried out in the pressurized tunnel from the German Dutch Wind facility (DNW-HDG). This tunnel was pressurized up to 80 bars to achieve high Reynolds numbers at small chord lengths (15 cm) and moderate tunnel speeds (M=0.1) This gives opportunity to isolate the Reynolds number effects from other combined effects that might come from e.g compressibility. Amongst others pressure distributions along the airfoil are measured with 90 pressure taps along the surface (including 5 high frequency pressure sensors), drag is derived from a wake rake and loads are measured with a 3 component balance. The chosen airfoil was a DU00-W-212. Airfoil selection was done from a list of airfoils including a few of NACA, FFA, DU and FX airfoils, considering the different transition behavior in pressure and suction side, a visible change in laminar drag bucket under different turbulent inflow conditions, the airfoil thickness and the amount of wind tunnel data from other facilities.

The measurements in the DNW-HDG wind tunnel are taken for Reynolds numbers ranging from 3 Million to 15 Million and brought into a public blind comparison test with calculations from parties inside and outside the AVATAR project. Moreover measurements in the wind tunnel from the partner LM were done on the DU00-W-212 airfoil of 900 mm chord for Reynolds numbers of 1.3, 3. 4. 5 and 6 Million where the latter Reynolds number was taken at a Mach number of 0.29. The instrumentation was largely similar to the experiment in the DNW-HDG e.g. pressure distributions are measured at locations similar to the locations of the pressure taps in the DNW-HDG experiment.

In the next section the DNW-HDG measurements are discussed in more detail and they are compared with the LM measurements for Reynolds numbers of 3 and 6M.

3.2. DNW-HDG measurements: Blind test results

The present section highlights a selection of DNW-HDG measurements on which a detailed description is given in [5]. This section only shows the Reynolds number dependency on the L/D

which is then compared to the calculated L/D from a blind comparison. In this blind comparison the following institutes and codes participated where a distinction is made between full CFD methods and panel methods.

	DTU	UAS-Kiel	NTUA	UoG	ForWind	USTUTT	ORE Catapult
Full CFD	Ellipsys	TAU	MAPFlow	HMB	OpenFoam		
Panel						XFOILvUSTUTT	XFOILv6.96

Most of the results included the modelling of boundary layer transition where EllipSys, TAU and the panel methods apply the e^N method. The HMB solutions employed the k-ω γ Re_θ transition model that yielded solutions with very early transition. The ForWind calculations are fully turbulent.

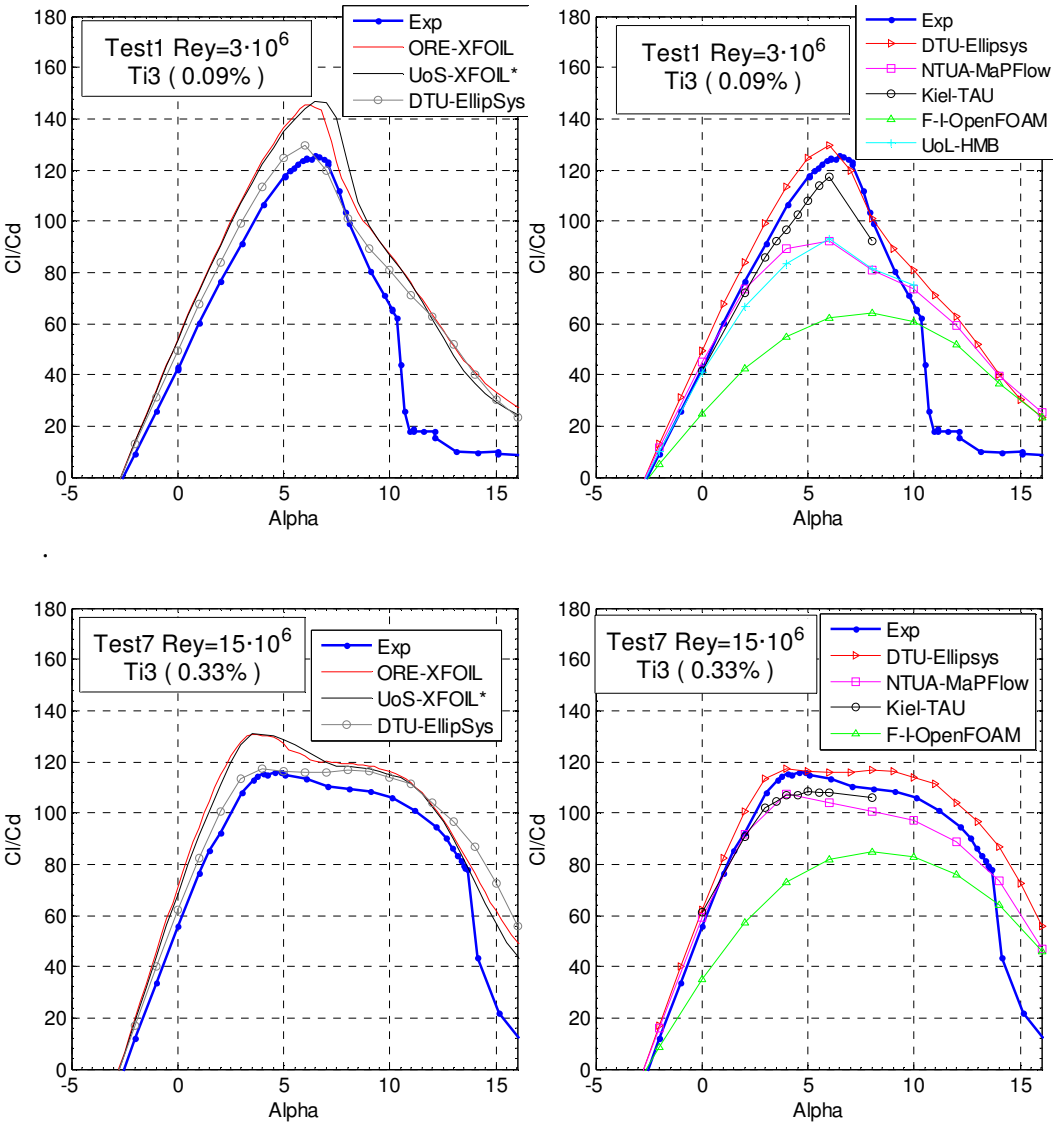

Figure 3. c_l/c_d as function of angle of attack measured and calculated, for Re=3M (upper) and 15M (lower), panel methods compared to EllipSys(left) and full CFD (right)

Figure 3 shows the results for a Reynolds number of 3M (upper) in comparison to a Reynolds number of 15 M(below) for the full CFD results (right) and the panel methods (left, note that the figures on panel methods also include EllipSys3D results for reference).
An important Reynolds number dependency in terms of a ''flattening'' of the $c_l/c_{d,max}$ peak at increasing Reynolds number can be observed. This flattening goes together with a lowering of the $c_l/c_{d,max}$. These trends have important design implications: Although the lower c_l/c_d reduces production, the wide peak with high values of c_l/c_d makes rotor operation less sensitive to the precise design point, i.e. the production at slight off-design conditions is enhanced.
Figure 3 shows that the trend is predicted well by those methods which use the so-called e^n boundary layer transition model. Other models resulted in early transition with results closer to fully turbulent solutions . In this respect reference can be made to [6] which shows a poor prediction of boundary layer transition at high Reynolds numbers using correlation based transition models.

3.3. Comparison DNW-HDG and LM measurements

In figure 4 the c_l/c_d versus angle of attack for the DU 00-W-212 airfoil as measured in the DNW-HDG tunnel is compared to the measurements at the LM wind tunnel. Results are shown for 2 Reynolds numbers: Re = 3 and 6 Million.

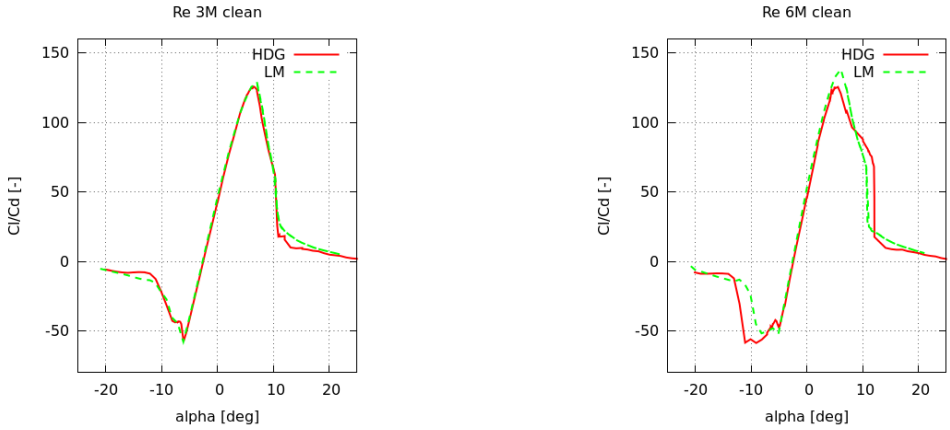

Figure 4. c_l/c_d as function of angle of attack measured in DNW-HDG and LM wind tunnel at Re = 3M (left) and 6M (right)

A very good agreement is found between the measurements from both wind tunnels. The main difference is seen near $(c_l/c_d)_{max}$ where the values measured in the LM wind tunnel are slightly higher. Near the stalling angle of 10 degrees some difference become apparent too. The differences are more pronounced at Re=6M.

In order to explain these differences it should be known that the Reynolds number in the LM and DNW-HDG test are similar but these Reynolds number are reached at different Mach numbers. This is a result of the fact that the Reynolds number in the DNW-HDG is largely controlled by pressure i.e. the velocity can be kept low where it is controlled by tunnel speed in the LM tunnel, leading to a higher Mach number in the LM experiments.
Moreover the turbulence level of the LM tunnel is known to be lower than the turbulence level of the DNW-HDG tunnel (0.05 vs 0.1% at Re=3M and 0.1 vs. 0.2 % at Re=6M). An analysis based on XFOIL calculations to be published in [19] shows that the minor differences in the 2 experimental campaigns can consistently be explained by the differences in tunnel conditions.

4. Modelling airfoil aerodynamics

Section 3.2 already touches upon the modelling of airfoil aerodynamics through the comparison of modelling results to the DNW-HDG experiments on the DU 00-W-212 airfoil.
Within AVATAR an extensive calculational benchmark has been carried for the airfoils and conditions along the AVATAR blade, see figure 2 which initially led to a large spread in computed results. To understand this spread a benchmarking study was carried out with various CFD codes where emphasis was put on the necessary domain sizes, grid resolutions and iterative convergence criteria in order to reach numerical consistent solutions at the relevant conditions, i.e. a low Mach number of 0.1 and Reynolds numbers ranging from 3 to 15 Million. The airfoil tested was again the DU 00-W-212 as used in the above mentioned wind tunnel tests.
The results from this study are discussed in detail in [16] and summarized in this section.

In the study 7 CFD codes were applied, including compressible and incompressible solvers. All applied codes are RANS with the k-ω SST turbulence model from Menter [17] with different transition models.

For the CFD simulations, a common series of grids were generated by using the HypGrid2D grid generator [18], all with an O-mesh topology and 384 times 192 cells in chord-wise and normal direction, with the outer boundary 40 chords away from the airfoil. To have an y+ value below 2 at all investigated Reynolds numbers a normalized off wall distance of $1.5x10^{-6}$ times the chord was chosen. The grid refinement study was then performed by simply removing every second point in the supplied grid. The left picture in figure 5 shows the supplied grid where the right picture shows the grid after two coarsenings.

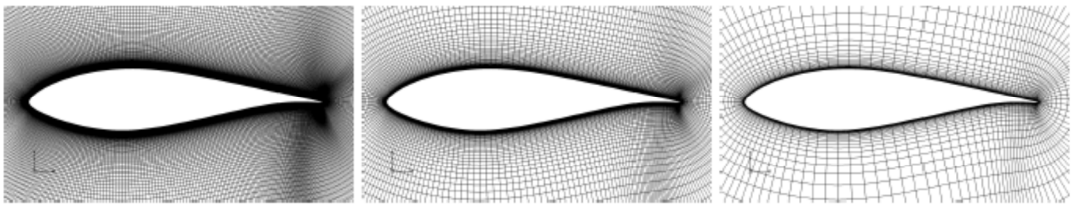

Figuur 5: Details of the grids near the surface, full grid(left) coarsened grid (right)

Most partners used this common grid but two partners decided to generate their own meshes where some partners tested additional meshes (C, OCH), grid resolutions and domain sizes to investigate the sensitivity of results on these parameters.

Eventually a good agreement in results from the various CFD solvers was found but only after several lessons were learned. Amongst others the high Reynolds requires very small cells at the wall in the order of $1.5x10^{-6}$ times the chord where the expansion rate in the high gradient regions should be limited e.g. by hyperbolic tangent stretching. It was also found that with the supplied O mesh and a domain size of 40 chords some solvers still needed a vortex correction to account for the induced velocity in the far field where other solvers needed such corrections when using different mesh topologies, e.g. the CH or OCH grids. Alternatively, to assure a domain size independent solution, the domain size can to be enlarged but this could need 100 chords. It was also found that the requirements to obtain grid independent solutions need to be considered at all (and not one) relevant angles of attack

where the requirements for a grid independent solution may differ from code to code even though all these codes are formally second order.

When sufficient attention is paid to all of the above mentioned aspects, the very different CFD solvers can provide glide ratios with differences below 2% for the turbulent cases, see figure 6.

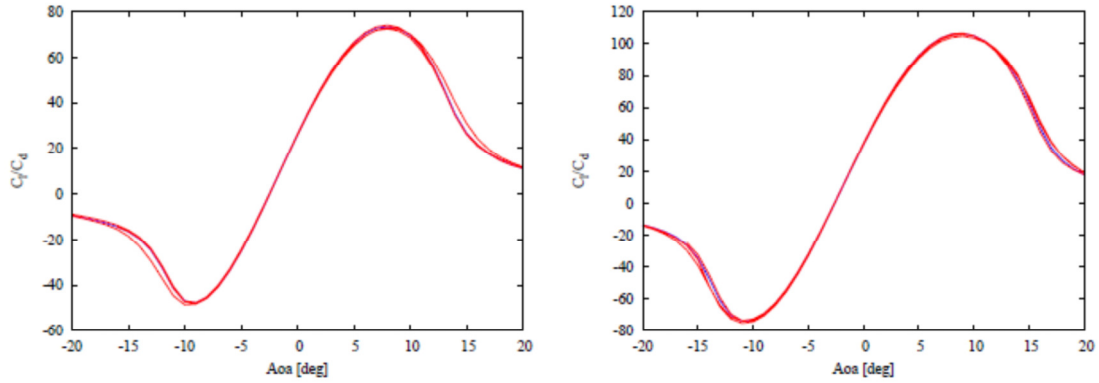

Figure 6: Glide ratio of grid converged results at Re = 3M (left) and 15M (right). Fully turbulent results

This was also found for the transitional cases if they are based on the e^N transition model in view of the problem mentioned in section 3.2 with the use of correlation based transition models at high Reynolds numbers. Obviously the good agreement in computed results does not guarantee that the solution is approximating the relevant physics but it is believed to assure that the solution is a true representation of the implemented models.

The lessons learned in this work will be guiding the computational work in 3D rotor simulations (Section 6).

5. Modelling of Flow Devices

Flow control devices are expected to be valuable solutions for improving the behaviour of modern wind turbine blades in terms of power production and loads, in particular for the 10MW+ turbines as considered in AVATAR. Therefore, one of the aims of the AVATAR project is to generate reliable simulation models and software tools to include flow control concepts on large wind turbine blades. The main devices which are considered in AVATAR are LE/TE flaps and vortex generators, the behaviour of which is assessed on sectional and rotor level. Root spoilers are assessed too

First, an extensive database of VGs and flaps has been generated of existing and new experimental data and CFD simulations. In order to develop and validate low/intermediate models for flow devices, a code to code comparison and a validation with experimental data is carried out. After confidence has been gained on these models, a parametric study has been performed in which the effect of design variables and operating conditions related to the flow control devices is evaluated on the aerodynamic response. It must then be noted that the amount of results on flow control devices generated within AVATAR is huge and the breadth of results makes it virtually impossible to summarize all finding within this paper. For that reason, a limited number of results on the parametric study for trailing edge flaps and vortex generators are highlighted. For more information reference is made to [8] until [12].

5.1. Parametric study

A parametric study is performed which aims to investigate the impact of some flow control design variables (e.g. dimensions and distribution along the blade) and operating conditions on the aerodynamic response of the airfoil and rotor. The parametric study also provides insights on the usefulness of the developed aerodynamic tools for practical applications.

First, a study was carried out which aimed to find the design parameters and operational conditions of flow control devices with maximum impact on the aerodynamic performance of rotors and blades. This study and a complete description of cases can be found in the corresponding deliverable of the AVATAR project [10]. The study focused on leading edge (LE) and trailing edge (TE) flap devices for load reduction and on vortex generators (vg's) for power increase. TE flaps are expected to have most potential for load reduction in attached flow conditions since a deployment of flap at the trailing edge affects lift more than a similar deployment at the leading edge. On the other hand, LE flaps are expected to have a good potential at unsteady separated flow / dynamic stall due to their effect on LE separation.

In the following list the airfoils are mentioned together with the flow control devices which have been used in the parametric study on sectional level. They are based on the airfoils found on the AVATAR and INNWIND.EU turbine for which calculations are done at the appropriate operational conditions.

- FFA W3 333 airfoil with VGs, applied at 35% span of the INNWIND.EU turbine with chord = 6.06 m
- DU-331 airfoil with VGs applied at 35% span of the AVATAR turbine with chord =5.84 m
- FFA W3 248 airfoil with LE flaps applied at 60% span of the INNWIND.EU turbine with chord = 4.43 m
- DU 240 airfoil with LE flaps applied at 60% span of the AVATAR turbine with chord = 4.36 m
- FFA W3 241 with TE flaps applied at 75% span of the INNWIND.EU turbine with chord = 3.31 m
- DU 240 airfoil with TE flaps applied at 75% span of the AVATAR turbine with chord = 3.45m

For the 3D study, the AVATAR and INNWIND RWTs are simulated with different configurations of VGs and TE flaps in the blades.

For the study of TE flaps, the effect of flap length, shape and angle is investigated, and the location and extension of the flap along the blade together with operating conditions, the reduced frequency of a flap oscillation and mean angle of attack. Two examples are shown in figures 7 and 8.

Figure 7 shows Δc_l i.e. the increase of c_l with respect to the case without flap, for different flap lengths, with a curvilinear TE flap at angle 10º in the DU240 airfoil at rated angle of attack (1º). The agreement between the codes is very good, showing a decreased effectivity with flap length. Figure 8 presents the F_x (out-of-plane force) along the blade radius of the INNWIND.EU rotor, in rated operating conditions, with a flap at 10º, where the flap extends over 10% blade radius centred in the 90% span station. The presence of the flaps is clear through an increase in force. Some differences between the codes are found in absolute load levels in both the area with and without flap but the relative force increase from the flaps is predicted similarly by the codes. More results related to the study of a TE flap can be found in [10]. This reference also includes results on leading edge flaps.

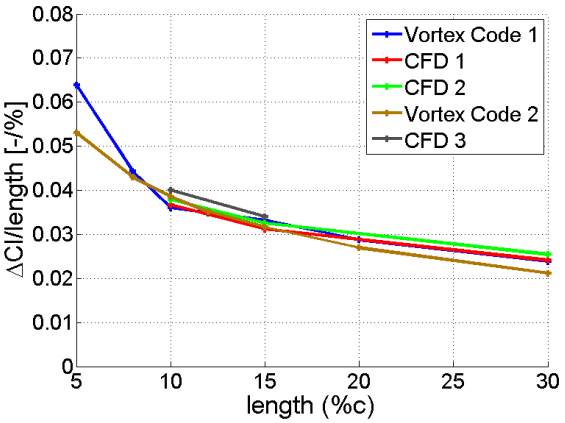

Figure 7: Increase of c_l per unit flap length at different flap lengths for the DU240 airfoil, at rated AoA, with a curved TE flap at flap angle=+10º

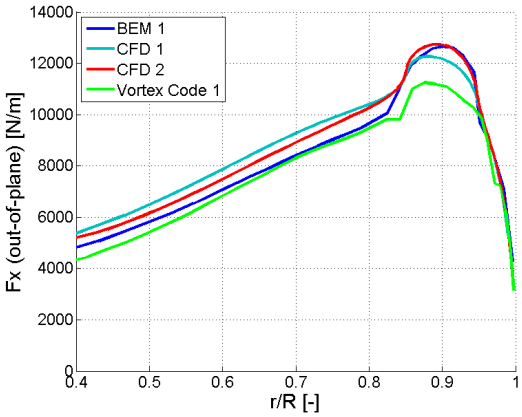

Figure 8: Fx (out-of-plane) along the blade for the InnWind.EU rotor, rated wind speed conditions, flap centred in the 90% radius extended over 10% span

The study on vg's considered the height, length, angle with respect to flow and internal and external distances, as well as the location and extension along the blade. Figures 9 and 10 show two examples. Figure 9 presents the increase of c_l (Δcl) from the vg's, at different configurations which represent different heights and chord locations on the FFA-W3-333 airfoil at rated angle of attack (8.8º) calculated by different codes, including CFD codes with so-called BAY implementations for the modelling of vg's [20]. The configuration numbers 1 to 9 along the x-axis refer to vg's located at 25% chord, and heights of 6, 10, 12, 15, 18, 24, 30, 36 and 60 mm respectively (where chord length = 6.06 meter). The configuration number 10 to 15, refer to vg's located at 30% chord, and heights of 9, 15, 18, 30, 36 and 60 mm respectively. Finally configuration numbers 16 to 24 refer to vg's located at 40% chord, and heights of 15, 17, 18, 30, 34, 36, 60, 68 and 90 mm respectively. In general, a clear increase of Δc_l with height is found, in particular for smaller heights. The dependency of Δc_l on chord position is less pronounced. Figure 10 shows the increase in the aerodynamic power of the AVATAR rotor at rated conditions with vg's centred at 35% blade radius and radial extensions ranging from 5 to 15%. For the operating conditions of the AVATAR rotor, the increase in power is limited, slightly more for larger radial extensions. The agreement of the codes is very good.

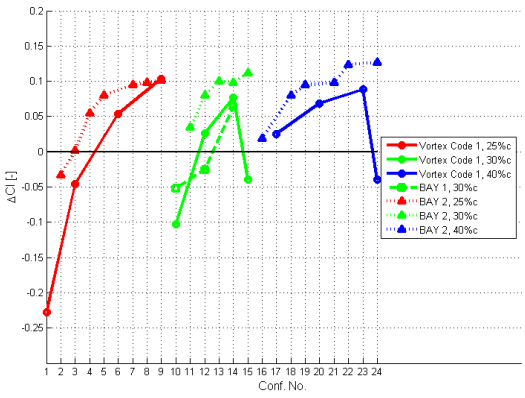

Figure 9: Increase of Cl with respect to the case without VGs, at rated AoA, for the FFA-W3-333 airfoil

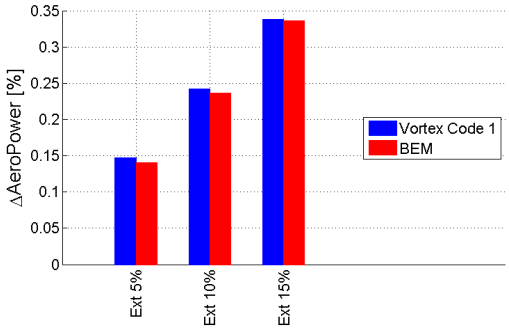

Figure 10: % change of power including VGs, AVATAR rotor simulation with BEM and vortex codes

Some interesting conclusions and guidelines for design have been obtained from this parametric study. One of the main conclusions is that the rotor design has significant influence on the performance of the flow control devices, indicating that design and use of flow control devices should be taken into account from the initial rotor design. Although not shown in this paper, a comparison between calculations and measurements on flow control devices revealed that the relative effect of flow devices is often modelled reasonably well in the sense that not much extra uncertainty is added from the modelling of flow devices to the uncertainty which already exists in the modelling of the clean configuration, in other words most of the discrepancies which is found in the modelling of flow devices was already apparent in the modelling of the clean conditions. However this observation is less true for the modelling of vg's (in particular the drag from vg's) which turns out be challenging. Detailed information with the justification of these conclusions can be found in [10].

6. Modelling rotor aerodynamics at yawed conditions

The previous sections mainly describe activities which refer to the modelling and measurements of sectional airfoil aerodynamics. The understanding of airfoil aerodynamics and the improvement of airfoil aerodynamic models are essential ingredients for the improvement of models needed to calculate the aerodynamics of the entire rotor.

Within AVATAR several calculational rounds are carried on the modelling of an entire rotor with and without flow devices and with and without aero-elastic effects at various conditions (e.g. yaw, partial wake, extreme shear). This section focusses on results which include aero-elastic effects. Initially most calculations in AVATAR included the effect of the controller which led to the unwanted side effect of a (slightly) different time response in pitch and/or rpm which in turn may yield a considerable different aerodynamic response if for example the initiation of an event takes place at a different azimuth angle. Such difference in aerodynamic response is then mainly related to the different rotor speed and only indirectly to the primary goal of AVATAR which is the assessment of aerodynamic modelling effects. This section therefore focusses on results obtained without controller from the ECN AeroModule [14] which is a code with an easy switch between the ECN-BEM models and the ECN-AWSM model where the latter is based on a free vortex wake method. Moreover a modified AWSM model is included which prescribes the wake and vortex convection velocities after a certain distance behind the rotor. The AeroModule is connected to the PHATAS structural solver [13]. In this way the aero-elastic response is calculated with largely the same input data but with 3 different aero-models in line with the AVATAR philosophy that engineering models are improved using results from more advanced methods. In this example the main difference between the aerodynamic models lies in the calculation of induction which is carried out in a more physical way with the vortex wake methods. The effects of airfoil aerodynamics are included in a similar way through airfoil coefficients as function of angle of attack (corrected for three dimensional effects in a similar way).
The more physical way of calculating induction will be important at e.g. yawed conditions for which results are presented in this section. The calculations are carried out on the INNWIND.EU RWT which is expected to be a more challenging case for the subject of induction aerodynamics, see section 2. The yaw angle is 30 degrees and a wind shear exponent of 0.2 is assumed at rated wind speed. Zero azimuth is defined at the 12 o' clock position for a clock-wise rotating turbine and yaw is defined such that the so-called downwind side of the rotor is between 0 and 180 degrees azimuth.

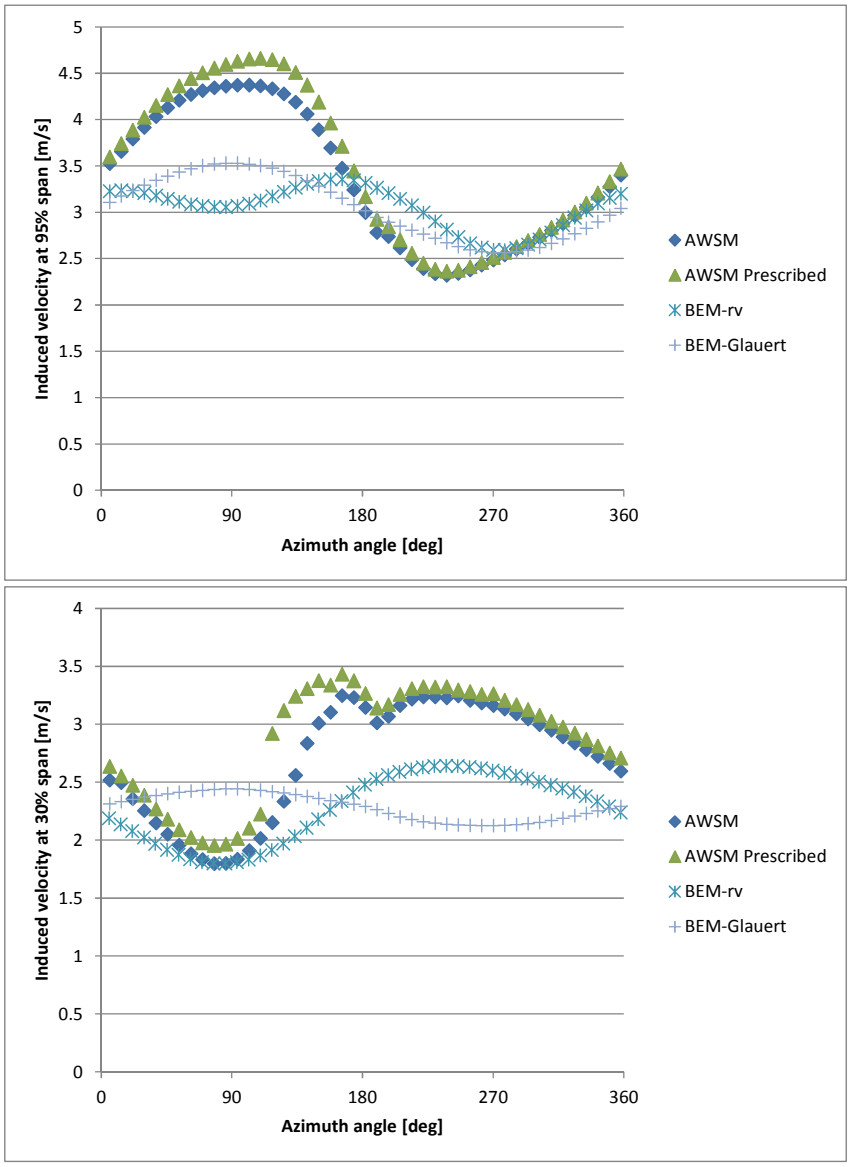

Figure 11: Induced velocity as function of azimuth angle at 95% span (top) and 30% span (bottom) for INNWIND.EU rotor

Figure 11 presents the axial induced velocities function of azimuth angle. It can be noted that 2 BEM models are included: A BEM-Glauert model which includes the standard Glauert model with a sinusoidal azimuthal variation of induced velocities all along the blade such that the maximum induced velocity appears at the downwind side of the rotor plane (between 0 and 180 degrees azimuth). Such sinusoidal variation is induced by tip vortices only. Moreover results are included from a modified model as described in [7] indicated with BEM-rv. This model was developed by ECN outside the framework of AVATAR by analysing hot wire measurements carried out in the Open Jet Facility of TUDelft [15]. It is more physical in the sense that it includes the effects from the root vortex which are not considered in the Glauert model. As such the azimuthal variation of the induced velocities at the root deviates from the sinusoidal behaviour induced by tip vortices, i.e. it leads to

maximum induced velocities at the upwind side of the rotor between 180 and 360 degrees azimuth where the minimum velocities are induced at the downwind side between 0 and 180 degrees

Although figure 11 shows that both BEM models generally underpredict the magnitude of the azimuthal variations compared to the vortex wake methods at 30% span, the qualitative agreement between the BEM-rv model and vortex wake models is good, i.e. the maximum velocity is induced at the upwind side and the minimum velocity is induced at the downwind side. The Glauert model fails to predict this trend, i.e. the maximum induced velocity is reached at the downwind side of the rotor plane as induced by a tip vortex wake only.

On the other hand it can be observed that the qualitative behaviour of the induced velocity at 95% span from the BEM-rv model compares slightly poorer to the vortex wake model in particular because the dip in induced velocity at an azimuth angle of 90 degrees as a result of the root vortex is still present. This offers room for improvement of ECN's yaw model by altering the radial dependency of the parameters in the model from [15] such that the effect of the root vortex is 'damped out' at 95% span. Hence the present comparison forms a nice example of how BEM models are going to be improved from more advanced models.

6.1. Canonical cases

It is noted that at a later stage of the project canonical cases have been defined. The aim of these cases is to condense differences to 'pure' aero modelling effects and to assess the weaknesses and the potential for modelling improvements, i.e. cases are initially carried out without controller, for a rigid construction and with prescribed inflow to which 'complications' (e.g. yaw, shear etc) are added in a systematic way. These results can then support the observations made in the previous sections on discrepancies between BEM and more advanced methods at e.g. yawed conditions

7. Conclusions

This paper presents the most recent results from the EU project AVATAR in which aerodynamic models are improved and validated for wind turbines on a scale of 10 MW and more. Measurements on a DU 00-W-212 airfoil are presented which have been taken in the pressurized DNW-HDG wind tunnel up to a Reynolds number of 15 Million. These measurements show a 'flattening' of the cl/cd peak towards high Reynolds numbers. The measurements have been compared with data obtained in the LM wind tunnel for Reynolds numbers of 3 and 6 Million. The mutual agreement in measurements is very good indicating a good measurement quality. The measurements are also compared with calculational results, which showed a good performance of the e^N transition model at high Reynolds numbers. Still CFD results on airfoil aerodynamics turned out to be challenging in the sense that initially a large scatter was found between the various models in the project. Eventually this scatter was reduced considerably after paying very careful attention to grid refinement and domain size in relation to grid topology. Moreover a selection is shown of activities which have been performed in AVATAR on the modelling and measurements of flow devices. The modelling of trailing edge flaps generally does not add much extra discrepancy to the discrepancies which already occur in the modelling of clean conditions but the modelling of vortex generators (in particular the drag from vortex generators) turns out to be challenging. Finally results are shown between results from 3D rotor models where a comparison is made between results from vortex wake methods and BEM methods from which recommendations for the improvement of the modelling yaw aerodynamics could be derived.

References

[1] Bak, C., Zahle, F., Bitsche, R., Kim, T., Yde, A., Henriksen, L., Hansen MH, Blasques JPAA, Gaunaa MA. Natarajan, M. H. *The DTU 10-MW Reference Wind Turbine* Danish Wind

Power Research 2013, Fredericia, Denmark, 27/05/2013

[2] Chaviaropoulos, T., Beurskens H.J, M., & Voutsinas, S. *Moving towards large(r) high speed rotors – is that a good idea?* 2013 EWEA Conference Proceedings. Vienna.

[3] G. Sieros, D. Lekou, D. Chortis, P. Chaviaropoulos, X. Munduate, A. Irisarri, H. Aa. Madsen, K. Yde, K. Thomsen, M. Stettner, M. Reijerkerk, F. Grasso, R. Savenije, G. Schepers, C.F. Andersen *AVATAR Reference Blade Design, AVATAR Deliverable 1.2,* http://www.eera-avatar.eu/ January 2015

[4] R. Quinn, B. Bulder, G. Schepers *An investigation into the effect of low induction rotors on the levelised cost of electricity for a 1GW offshore wind farm* EERA-Deepwind conference, Trondheim, January 2016

[5] O Pires, X Munduate , O Ceyhan , M Jacobs , H Snel *Analysis of high Reynolds numbers effects on a wind turbine airfoil using 2D wind tunnel test data* Science of Making Torque 2016,

[6] Niels N. Sørensen, F. Zahle , J.A. Michelsen *Prediction of airfoil performance at high Reynolds numbers* EFMC 2014, Copenhagen, September 2014,

[7] J.G. Schepers *Engineering models in aerodynamics*, PhD thesis, November 27th, 2012, Technical University of Delft, Netherlands, ISBN 9789461915078

[8] M. Manolesos, J. Prospathopoulos, Gonzalez, A., Aparicio, M., Méndez, B., Gómez-Iradi, S., Munduate. X., Chaviaropoulos, T. Barlas, A., Garcia N. R., Sorensen, N. N. Barakos, G., Wang, Y. Jost, E., Chasapogiannhs, P., Diakakis, K., Papadakis, G, Voutsinas, S. Baldacchino, D. *CFD and experimental database of flow devices, comparison*, *AVATAR Deliverable 3.1*, http://www.eera-avatar.eu/ February 2015

[9] Ferreira, C., Gonzalez, A., Baldacchino, D., Aparicio, M., Gómez, S., Munduate. X., Barlas, A., Garcia N. R., Sorensen, N. N., Troldborg, N., Barakos, G., Jost, E., Knecht, S., Lutz, T., Chassapoyiannis, P., Diakakis, K., Manolesos, M, Voutsinas, S., Prospathopoulos, J., Gillebaart, T., Florentie, L., van Zuijlen, A., Reijerkerk, M. *Task 3.2 : Development of aerodynamic codes for modelling of flow devices on aerofoils and rotors*, *AVATAR Deliverable 3.1*, http://www.eera-avatar.eu/ November 2015

[10] M. Aparicio, A. Muñoz, R. Martín, A. Gonzalez Méndez, B., Gómez-Iradi, S., Munduate, X. Jost, E., Lutz, T. Barakos, G., Colonia, S. Florentie, L. Caboni, M. Ramos-García, N., Troldborg, N., Sørensen, N. Prospathopoulos, J., Chassapoyiannis, P., Manolesos, M., Diakakis, K., Voutsinas, S. Stettner, M. *Deliverable 3.3: Results of a parametric study of flow devices, guidelines for design*, *AVATAR Deliverable 3.1*, http://www.eera-avatar.eu/ April 2016

[11] C. Fereira, *Results of the AVATAR project for the validation of 2D aerodynamic models with experimental data of the DU95W180 airfoil with unsteady flap* Science of Making Torque, October 2016

[12] D Baldacchino, M Manolesos, C Ferreira , A Gonzalez Salcedo, M Aparicio, T Chaviaropoulos, K Diakakis, L Florenti , N R. Garcıa , G Papadakis , N N. Sørensen , N Timmer , N Troldborg , S Voutsinas and A van Zuijlen *Experimental benchmark and code validation for airfoils equipped with passive vortex generators*, Science of Making Torque, October 2016

[13] C. Lindenburg *Comparison of PHATAS Versions and the Wind turbine Module* ECN-E--11-066, 2011

[14] Boorsma, K.; Grasso, F.; Holierhoek, J.G. *Enhanced approach for simulation of rotor aerodynamic loads*, ECN-M--12-003, 2012

[15] J.G. Schepers *An engineering model for yawed conditions developed on basis of wind tunnel measurements*, In proceedings of ASME Wind Energy Symposium held at Reno USA, January 1999

[16] N. Sørensen, B. Mendez, A. Munoz, G. Sieros, E. Jost, T. Lutz, G. Papadakis, S. Voutsinas, G. Barakas, S. Colonia, D. Baldacchino, C. Baptista, C. Ferreira *CFD comparison for 2D flow* Science of Making Torque, October 2016

[17] F.R. Menter *Zonal 2 equation k-ω Turbulence models for aerodynamic flows*. AIAA paper

1993-2906, 1993

[18] N. N. Sørensen. *HypGrid2D a 2-D Mesh Generator*. Risø-R- 1035-(EN), Risø National Laboratory, Roskilde, Denmark, Feb 1998.

[19] O.Pires, X.Munduate, O.Ceyhan, M.Jacobs, J.Madsen, J.G. Schepers *Analysis of the high Reynolds number 2D tests on a wind turbine airfoil performed at two different wind tunnels* To be published at EWEA Annual Event, September 2016

[20] Bender, E.E., Anderson, B.H., Yagle, P. (1999). *Vortex Generator Modelling for NavierStokes Codes*. In 3rd Joint ASME/JSME Fluids Engineering Conference, San Francisco, CA., number March